

## Phase equilibrium in manganites under a magnetic field studied using a two-orbital model

This article has been downloaded from IOPscience. Please scroll down to see the full text article.

2006 J. Phys.: Condens. Matter 18 L171

(<http://iopscience.iop.org/0953-8984/18/15/L02>)

View [the table of contents for this issue](#), or go to the [journal homepage](#) for more

Download details:

IP Address: 129.252.86.83

The article was downloaded on 28/05/2010 at 09:21

Please note that [terms and conditions apply](#).

## LETTER TO THE EDITOR

# Phase equilibrium in manganites under a magnetic field studied using a two-orbital model

S Dong<sup>1</sup>, X Y Yao, K F Wang and J-M Liu

Nanjing National Laboratory of Microstructures, Nanjing University, Nanjing 210093,  
People's Republic of China

and

International Centre for Materials Physics, Chinese Academy of Sciences, Shenyang,  
People's Republic of China

E-mail: [saintdosnju@gmail.com](mailto:saintdosnju@gmail.com)

Received 11 February 2006

Published 30 March 2006

Online at [stacks.iop.org/JPhysCM/18/L171](http://stacks.iop.org/JPhysCM/18/L171)

## Abstract

The phase equilibrium in manganites under a magnetic field is studied using a two-orbital model, based on the equivalent chemical potential principle for competitive phases. We focus on the magnetic field induced melting process of the charge exchange (CE) phase in half-doped manganites. It is predicted that the homogeneous CE phase will begin to decompose into a coexisting ferromagnetic phase and CE phase once the magnetic field exceeds the threshold field. More quantitatively, the volume fractions of the two competitive phases in the phase separation regime are evaluated.

(Some figures in this article are in colour only in the electronic version)

## 1. Introduction

Manganites, a typical class of strongly correlated electron systems, have been intensively studied in the last decade, due to their unusual behaviours such as colossal magnetoresistance (CMR) and potential applications. The double-exchange (DE) mechanism can explain the magnetic transition qualitatively, but the more complex mechanism responsible for the CMR is not yet fully understood. The idea of phase separation (PS) was recently proposed to explain the essential physics underlying the amazing behaviours of manganites, while more and more theoretical and experimental evidence confirms the existence of PS due to the intrinsic inhomogeneity [1–3].

Earlier investigations on the phase diagram of manganites revealed the first-order character of the phase transitions between various phases, e.g. charge-ordered (CO) insulator and ferromagnetic (FM) metal [2, 4–6]. The insulator–metal transition in manganites can be

<sup>1</sup> Author to whom any correspondence should be addressed.

reasonably well understood as the consequence of percolation of FM metal filaments embedded in the insulated matrix, and there is plenty of experimental evidence to support this PS framework [2, 7, 8]. Current theories on manganites mainly stem from the competition between several interactions: DE, superexchange, Hund coupling, electron–phonon interaction and Coulomb interaction [2]. Besides this, the effect of quench disorder on PS dynamics is highlighted, especially that on the large scale PS. Theoretical progress has enabled us to sketch the phase diagram in some special regimes from calculations and identify the PS regime in parameter space, with various microscopic models [9–11]. Nevertheless, it is still unclear theoretically how the PS develops, especially under an external perturbation, e.g. magnetic or electric field. In other words, it is of interest to not only identify the existence of a PS regime, but also to find how the phase separation occurs and how it evolves upon external perturbation, because potential applications call for more adequate theoretical interpretation. For instance, the CMR effect, which is one of the most attractive topics in the physics of manganites, may be described using the resistor network model phenomenologically, on the basis of the percolation mechanism. In such cases the volume fraction of the metal phase is the key input variable, which, however, lacks a credible theoretical investigation as yet. In earlier studies, this important variable was obtained from experiments or toy models [12, 13].

## 2. Two-orbital model

First, a simplified two-orbital model will be introduced. Although it was explicitly solved in earlier work [14, 15], a brief description remains necessary here for completeness of consideration of the phase equilibrium (PE). The model Hamiltonian is

$$H = - \sum_{i\alpha\gamma\gamma'\sigma} t_{\gamma\gamma'}^\alpha d_{i\gamma\sigma}^+ d_{i+\alpha\gamma'\sigma} - J_H \sum_i \mathbf{s}_i \cdot \mathbf{S}_i + J_{AF} \sum_{(i,j)} \mathbf{S}_i \cdot \mathbf{S}_j \quad (1)$$

where  $\alpha$  is the vector connecting nearest-neighbour (NN) sites;  $d_{i\gamma\sigma}^+$  ( $d_{i+\alpha\gamma'\sigma}^+$ ) is the generation (annihilation) operator for the  $e_g$  electron with spin  $\sigma$  in the  $\gamma$  ( $\gamma'$ ) orbital on site  $i$  ( $i+\alpha$ );  $t_{\gamma\gamma'}^\alpha$  is the amplitude of NN hopping between  $\gamma$  and  $\gamma'$  orbitals ( $d_{x^2-y^2}$  as the  $a$  orbital,  $d_{3z^2-r^2}$  as the  $b$  orbital) along the  $\alpha$  direction, with  $t_{bb}^z = t_0 > 0$  ( $t_0$  is taken as the energy unit),  $t_{aa}^x = t_{aa}^y = \frac{3}{4}t_0$ ,  $t_{bb}^x = t_{bb}^y = \frac{1}{4}t_0$ ,  $t_{ab}^y = t_{ba}^y = -t_{ab}^x = -t_{ba}^x = \frac{\sqrt{3}}{4}t_0$ ,  $t_{aa}^z = t_{ab}^z = t_{ba}^z = 0$ ;  $\mathbf{S}_i$  is the spin operator for the  $t_{2g}$  core on site  $i$ , while  $\mathbf{s}_i$  is that for the  $e_g$  itinerant electron. The first term represents the kinetic energy (DE process) which leads to FM spin arrangement. The second term is the Hund coupling of  $e_g$  and  $t_{2g}$  electrons where  $J_H > 0$  is large enough to be regarded as infinite, so the spin of the  $e_g$  electron is always parallel to the same-site  $t_{2g}$  spin. The final superexchange interaction  $J_{AF} > 0$  favours coupling the NN  $t_{2g}$  spins antiferromagnetically.

The above simplified Hamiltonian can be solved exactly once a prior  $t_{2g}$  spin pattern is given. In real manganites, various  $t_{2g}$  spin patterns exist corresponding to abundant phases, e.g. FM, antiferromagnetic (AFM), CO, orbital-ordered (OO) phases. In this work, several typical  $t_{2g}$  patterns confirmed from experiments: C-type AFM (CAFM), G-type AFM (GAFM), FM and CE phases are chosen as the candidates to compare. The CAFM phase is constructed from antiferromagnetically coupled one-dimensional FM lines, while the CE phase is constructed from antiferromagnetically coupled one-dimensional zigzag FM chains and is found to be CO/OO [15–17]. The GAFM phase takes on the familiar AFM arrangement in all three directions. Then the Hamiltonian can be exactly solved when the Hund factor  $J_H$  is simplified as infinite. The procedure of derivation is straightforward and the detail can be found in [2]. Then density of states (DOS,  $D(E)$ ) of these phases can be calculated from the dispersion relationship using a numerical method, as shown in figure 1(a). In addition, the chemical potential  $\mu$  of these phases is obtained simultaneously by integrating the DOS, as

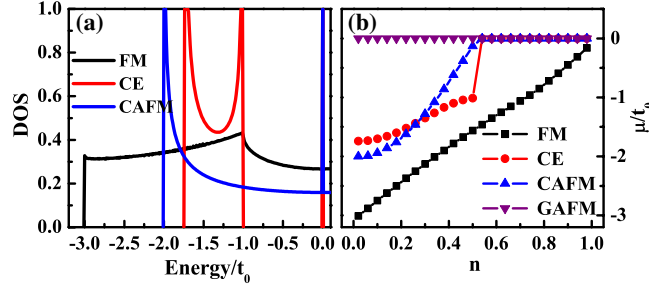


**Figure 1.** (a) Density of states of  $e_g$  electrons of the FM/CE/CAFM phase. Here only the regime  $E \leq 0$  is displayed since the symmetrical  $E > 0$  part is empty in the ground state. In the GAFM phase, there is only a single energy level at 0 because of the localization of  $e_g$  electrons. (b) Chemical potential  $\mu$  as a function of  $e_g$  electron concentration. The energy gap  $t_0$  for the CE phase at  $n = 0.5$  is evident both in (a) and in (b).

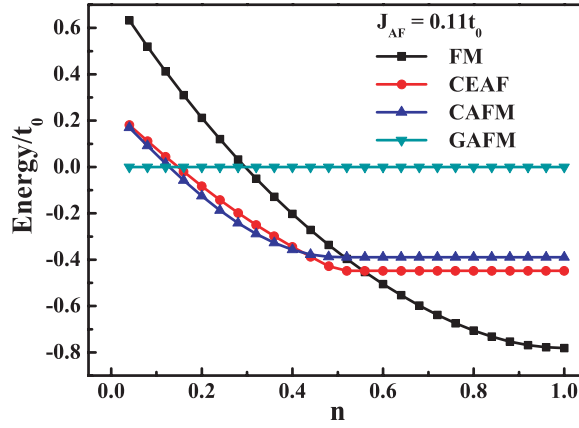


**Figure 2.** System energy  $E$  (ground state under zero field) as a function of  $e_g$  electron concentration  $n$ , with  $J_{AF} = 0.11t_0$ . Upon increasing the  $e_g$  electron concentration  $n$ , a transition sequence of the ground state: GAFM  $\rightarrow$  CAFM  $\rightarrow$  CE  $\rightarrow$  FM, occurs, as shown. The CE phase is possible as a ground state only in the narrow regime around the half-filling point.

shown in figure 1(b). Consequently, the ground state energy is calculated. For instance, the energy of the FM phase per site can be written as

$$E(n, H) = \int^{E < \mu} D(E)E dE + 3J_{AF}SS - gHS. \quad (2)$$

Here the first integral term gives the energy of the  $e_g$  electron; the second term arises from the NN FM correlation (three bonds per site) between  $S = 3/2 t_{2g}$  cores in the classical approximation; the last one is the Zeeman energy with the Landé factor  $g = 2$ . Besides this, the influence of  $H$  on  $D(E)$  should also be taken into account. The average  $e_g$  electron concentration  $n \in [0, 1]$ . The DOS, chemical potential and ground energy of other phases can also be calculated exactly, just as in the FM case.

However, what should be noted is that none of these phases can be stable over the whole doping range. In order to determine which phase is the preferred one at a given concentration  $n$ , the ground state energy of these phases, when  $J_{AF}$  is set as  $0.11t_0$  and  $H = 0$ , is plotted in figure 2. The preferred ground state is the energy minimal state. It should be GAFM as  $n \sim 0$ , because the interaction is almost pure AFM superexchange. As  $n \sim 0.3$ , the

preferred state is CAFM. The CE phase can appear only in a narrow regime,  $n \sim 0.5$ . When the gain from kinetic energy suppresses the loss of superexchange energy in the large  $n$  regime, the FM phase becomes the stable phase. With this calculation, the phase diagram over the whole concentration regime can be developed. Of course, the phase diagram of real manganites is more complex than this simple sketch for two reasons: first, the Hamiltonian (1) is oversimplified; and secondly the candidate phases chosen here are not a complete list but just four phases. However, the calculated phase diagram is quite similar to that of some typical manganites (at zero temperature): e.g.  $\text{Nd}_{1-x}\text{Sr}_x\text{MnO}_3$  (here  $n = 1 - x$ ) [18]. In fact, it is shown that the phase diagrams of other manganites, e.g.  $\text{La}_{1-x}\text{Sr}_x\text{MnO}_3$  and  $\text{Pr}_{1-x}\text{Ca}_x\text{MnO}_3$ , can be reproduced roughly by adjusting the value of  $J_{\text{AF}}$ , whose role will be revisited below. An important truth revealed here is that no matter what  $J_{\text{AF}}$  is, the CE phase can either appear in the narrow regime  $n \sim 0.5$  or simply be unstable over the whole concentration regime.

### 3. Calculation of the phase equilibrium

First, we investigate the PE based on the above results from the two-orbital model. We emphasize particularly the evolving of the PS upon magnetic field perturbation. So we call it PE instead of PS in this work.

Here, a simple but representative case: the PE between the FM phase and CE phase with  $n = 0.5$ , will be studied. It corresponds to the melting process of a type of CO state (here it is the CE phase) under an external magnetic field. Since for the metallic phase the lattice distortions are absent and the  $e_g$  electrons are delocalized [19], the electron–phonon coupling and on-site Coulomb repulsion are unimportant. On the other hand, the CE phase can also be reasonably described as a band insulator using this Hamiltonian for the  $n = 0.5$  case [2, 15]. Therefore, (1) is suitable for dealing with the PE between the FM metallic phase and CE phase, noting that (1) can be exactly solved without scale issues.

The condition for PE in a PS system is the equivalence in chemical potential between the competitive phases, i.e. FM and CE, to be considered. From the above calculation (figure 1(b)), it is seen that at  $n = 0.5$  and under zero field, the chemical potential of  $e_g$  electrons in the pure FM phase is about  $-1.52t_0$  and that in the CE phase is  $-t_0$ . Therefore, the chemical potential  $\mu$  of  $e_g$  electrons for the possible PS system would be in the range  $[-1.52t_0, -t_0]$ . The sum of  $e_g$  electrons in the FM and CE phases can be calculated:

$$n_A = p_A \int^{E < \mu} D(E) dE \quad (3)$$

where  $p_A$  is the volume fraction of the A (FM/CO) phase. The upper limit of the integral should meet the equivalent chemical potential condition:  $\mu_{\text{FM}} = \mu_{\text{CE}} = \mu$ . Then the following set of equations yields

$$\begin{aligned} p_{\text{FM}} + p_{\text{CE}} &= 1 \\ n_{\text{FM}} + n_{\text{CE}} &= 0.5. \end{aligned} \quad (4)$$

By a numerical method, (4) can be solved with the prior assumed  $\mu$ . Given parameters  $J_{\text{AF}} = 0.11t_0$  and  $H = 0$ , the calculated relative volume fractions of the FM phase and CE phase as a function of  $\mu$  are shown in figure 3(a) (right axis). Besides the equivalence in chemical potential of  $e_g$  electrons, the condition for a stable PS state is the minimization of the energy of the whole system (including both  $e_g$  and  $t_{2g}$  electrons). Then by including the factor  $p_A$  into the energy equation, the total system energy (energy of all  $e_g$  and  $t_{2g}$  electrons at zero temperature)  $E = p_{\text{FM}}E_{\text{FM}} + p_{\text{CE}}E_{\text{CE}}$  can be calculated, as shown in figure 3(a) (left axis). It is seen that both  $p_{\text{FM}}$  and  $E$  are monotonically decreasing functions of  $\mu$ . The ground state must be the

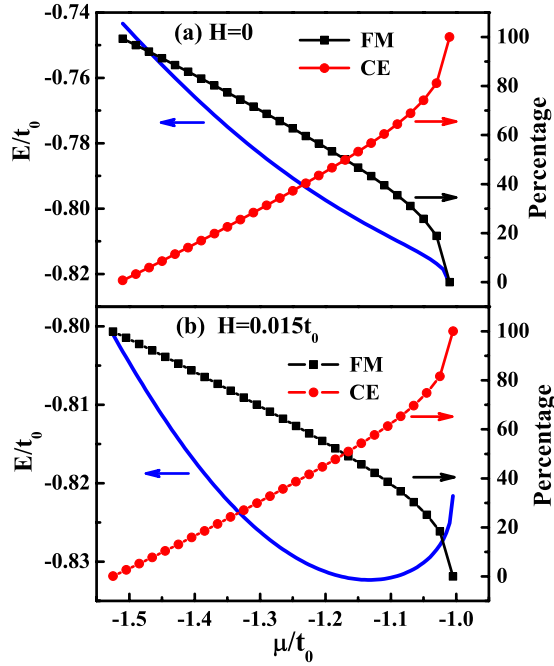


**Figure 3.** Volume fraction of the FM/CE phase (right axis) and corresponding total system energy  $E$  (left axis) as a function of the  $e_g$  chemical potential  $\mu$ .  $J_{AF} = 0.11t_0$ . (a) Zero-field case, where the ground state is the CE phase without phase separation because the energy decreases monotonically with the FM phase fraction; (b) under a magnetic field  $H = 0.015t_0$ , where an energy minimum appears at  $\mu = -1.13t_0$ . The coexistence with the fraction of FM and CE phases at this point is the ground state.

homogeneous CE phase because the PS state goes against the energy. In the case of nonzero magnetic field (e.g.  $H = 0.015t_0$ ), the above calculation is repeated by taking the magnetic field contribution to the DOS and energy into account. The results are plotted in figure 3(b). Interestingly, a nonzero field results in a minimum in the  $E-\mu$  curve (here at  $\mu \sim -1.13t_0$ ). The PS state associated with this minimal energy point is more stable than the homogeneous FM or CE phase. The value  $-1.13t_0$  is the real chemical potential of  $e_g$  electrons in this PS ground state which consists of 57% CE phase and 43% FM phase.

By varying the value of  $H$ , one can repeat the above calculation and then obtain the relative volume fractions of the two phases as a function of  $H$ , as shown in figure 4(a). When  $H$  is low (below the lower threshold  $H_{\min} \sim 0.0069t_0$ ), the CE phase is robust against magnetic field perturbation, indicating the stable and homogeneous CE phase as the ground state. Upon increasing of  $H$  beyond  $H_{\min}$ , part of the CE phase begins to melt into an FM phase, and  $p_{CE}$  will become less when the magnetic field  $H$  is higher under the equivalent chemical potential condition  $\mu_{FM} = \mu_{CE} = \mu$ . In detail, it is observed that the volume fraction of the FM phase increases rapidly once  $H > H_{\min}$ , and the growth becomes slower when  $H$  is even higher, as shown in figure 4(a). Note here that the threshold of percolation for the FM phase can be easily surpassed under a field slightly higher than  $H_{\min}$ . For instance, only a field of  $H = 0.009t_0$  is needed to obtain an FM phase of 24.7% (threshold for a three-dimensional simple cubic bond percolation), beyond which an insulator–metal transition may be expected. When  $H$  is extremely high (not shown in figure 4(a)), the condition for PE can no longer be satisfied, indicating a termination of the PS state, and the ground state will be the homogeneous FM state.

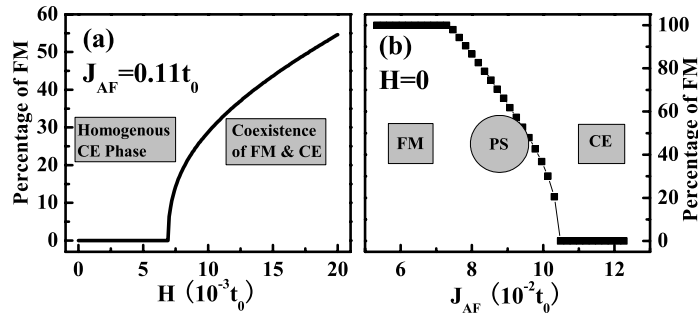


**Figure 4.** (a) Melting process of the CE phase under a magnetic field. When the field is below the threshold  $H_{\min}$ , the homogeneous CE phase is robust. Then phase separation occurs when  $H > H_{\min}$ . (b) Phase transitions induced by  $J_{AF}$  under zero-field conditions: the FM phase at weak  $J_{AF}$ ; coexistence of FM and CE phases at intermediate  $J_{AF}$ ; the CE phase at strong  $J_{AF}$ .

#### 4. Discussion

The above calculation indicates that the lower threshold of the magnetic field for melting the CE phase is  $0.0069t_0$ . Considering that  $t_0$  for low bandwidth manganites is small, e.g. 0.1 eV, the calculated  $H_{\min}$  is about 12 T, a value consistent with the experimental data [20–23]. Note here that  $H_{\min}$  is not equal to the direct energy gap between the FM and CE phase which is one order of magnitude larger than the experimental value (shown in figure 2; about  $0.08t_0$ ). This means that the magnetic field required to destroy the CO insulator is strongly reduced by PS which can occur once the energies of competitive phases are close to each other. On the other hand, as identified earlier, parameter  $J_{AF}$  plays a key role in PS although it is the least intrinsic interaction in manganites [2]. Other than in the above case of field induced sequences, abundant phenomena associated with PS in manganites can be predicted by our model through adjusting the parameter  $J_{AF}$ . For example, again at  $n = 0.5$ , a coexistence of the FM phase and CE phase under zero field is predicted at  $0.076t_0 < J_{AF} < 0.10t_0$ . When  $J_{AF}$  is further reduced, a homogeneous FM phase as the ground state is possible even under zero field. The transitions between three regimes: homogeneous FM state to phase separated state to homogeneous CE state, are identified, as presented in figure 4(b). These transitions can be mapped to real manganites of wide band to those of intermediate band and then those of narrow band [2]. In addition, because the value of  $S$  was normalized as 1 in former work without a magnetic field [15], the parameter comparison should be carried out using  $J_{AF}SS$  instead of  $J_{AF}$ . In this way, the  $J_{AF}$  regime in this work is consistent with that in earlier work [2]. Considering the PS, it is not strictly correct to determine the  $J_{AF}$  threshold by directly comparing the energies of the FM phase and CE phase [15].

It should be mentioned that the only parameter adjustable here is the superexchange  $J_{AF}$ , and the energy difference between different phases is dependent on the ratio  $J_{AF}/t_0$ . This is obviously oversimplified, referring to real manganites materials in which not only the double exchange/superexchange but also the Jahn–Teller distortion and Coulomb repulsion play important roles. For instance, the Jahn–Teller distortion in the CE phase will affect the energy band and DOS [24, 25]. In addition, although the phase diagram given in figure 2 is quite similar to those for some manganites, there are still some shortcomings. For instance, a prediction of the correct concentration  $n$  corresponding to the A-type AFM phase observed in  $\text{LaMnO}_3$  ( $n \sim 1.0$ ) [16] or  $\text{Nd}_{1-x}\text{Sr}_x\text{MnO}_3$  ( $x \sim 0.55$ ) [18] cannot be given by the present model. However, if a complete Hamiltonian is employed, the calculation has to be

oversimplified, e.g. limited to a small cluster, which is disadvantageous for dealing with PS. Fortunately, equation (1) in the present work can describe the FM/CE phase to a reasonably satisfactory extent and it is a good starting point for investigating the PE issue in PS systems with external magnetic field perturbation. Furthermore, the present approach represents a general roadmap for investigating the PE issues for manganites: e.g. phase competition other than the FM–CE one, of more than two phases, of different  $e_g$  concentrations, and the effect of perturbations other than a magnetic field etc. The key condition is the equivalence of chemical potential between competitive phases.

## 5. Conclusions

In summary, the principle of chemical potential equivalence has been introduced to investigate the phase equilibrium of half-doped manganites under an external magnetic field. By employing a two-orbital model, we have presented an explicit solution for the phase equilibrium between the FM phase and CE phase. The magnetic field threshold required for melting the CE phase has been calculated, and found to be consistent with the experimental results. The volume fractions of the two competitive phases in the phase separation regime as a function of the external magnetic field have been evaluated. In addition, the superexchange modulated transitions between ferromagnetic, phase separated and CE states under zero field are predicted.

S Dong thanks G X Cao for valuable discussions. This work was supported by the Natural Science Foundation of China (50332020, 10021001, 10474039) and National Key Projects for Basic Research of China (2002CB613303, 2004CB619004).

## References

- [1] Dagotto E 2005 *Science* **309** 257–62
- [2] Dagotto E 2002 *Nanoscale Phase Separation and Colossal Magnetoresistance* (Berlin: Springer)
- [3] Uehara M, Mori S, Chen C H and Cheong S W 1999 *Nature* **399** 560–3
- [4] Loudon J C, Mathur N D and Midgley P A 2002 *Nature* **420** 797–800
- [5] Murakami S and Nagaosa N 2003 *Phys. Rev. Lett.* **90** 197201
- [6] Aliaga H, Magnoux D, Moreo A, Poilblanc D, Yunoki S and Dagotto E 2003 *Phys. Rev. B* **68** 104405
- [7] Zhang L, Israel C, Biswas A, Greene R L and Lozanne A D 2002 *Science* **298** 805–7
- [8] Tokunaga M, Song H, Tokunaga Y and Tamegai T 2005 *Phys. Rev. Lett.* **94** 157203
- [9] Yunoki S, Hu J, Malvezzi A L, Moreo A, Furukawa N and Dagotto E 1998 *Phys. Rev. Lett.* **80** 845–8
- [10] Yunoki S, Moreo A and Dagotto E 1998 *Phys. Rev. Lett.* **81** 5612–5
- [11] Yunoki S, Hotta T and Dagotto E 2000 *Phys. Rev. Lett.* **84** 3714–7
- [12] Mayr M, Moreo A, Vergés J A, Arispe J, Feiguin A and Dagotto E 2001 *Phys. Rev. Lett.* **86** 135–8
- [13] Dong S, Zhu H, Wu X and Liu J M 2005 *Appl. Phys. Lett.* **86** 022501
- [14] Brink J v d and Khomskii D 1999 *Phys. Rev. Lett.* **82** 1016–9
- [15] Brink J v d, Khaliullin G and Khomskii D 1999 *Phys. Rev. Lett.* **83** 5118–21
- [16] Wollan E O and Koehler W C 1955 *Phys. Rev.* **100** 545–63
- [17] Goodenough J B 1955 *Phys. Rev.* **100** 564–73
- [18] Kajimoto R, Yoshizawa H, Kawano H, Kuwahara H, Tokura Y, Ohoyama K and Ohashi M 1999 *Phys. Rev. B* **60** 9506–17
- [19] Ahn K H, Lookman T and Bishop A R 2004 *Nature* **428** 401–4
- [20] Kuwahara H, Tomioka Y, Asamitsu A, Moritomo Y and Tokura Y 1995 *Science* **270** 961–3
- [21] Tomioka Y, Asamitsu A, Kuwahara H, Moritomo Y and Tokura Y 1996 *Phys. Rev. B* **53** R1689–92
- [22] Tokunaga M, Miura N, Tomioka Y and Tokura Y 1998 *Phys. Rev. B* **57** 5259–64
- [23] Okimoto Y, Tomioka Y, Onose Y, Otsuka Y and Tokura Y 1999 *Phys. Rev. B* **59** 7401–8
- [24] Brey L 2005 *Phys. Rev. B* **71** 174426
- [25] Dong S, Dai S, Yao X Y, Wang K F, Zhu C and Liu J M 2006 *Phys. Rev. B* **73** 104404 (Preprint cond-mat/0508673)